

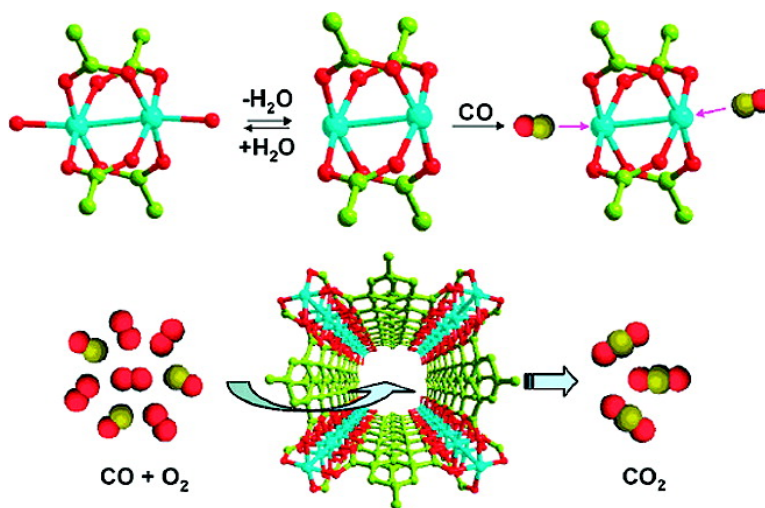
Communication

Probing the Lewis Acid Sites and CO Catalytic Oxidation Activity of the Porous Metal–Organic Polymer [Cu(5-methylisophthalate)]

Ru-Qiang Zou, Hiroaki Sakurai, Song Han, Rui-Qin Zhong, and Qiang Xu

J. Am. Chem. Soc., **2007**, 129 (27), 8402-8403 • DOI: 10.1021/ja071662s • Publication Date (Web): 19 June 2007

Downloaded from <http://pubs.acs.org> on February 16, 2009



More About This Article

Additional resources and features associated with this article are available within the HTML version:

- Supporting Information
- Links to the 16 articles that cite this article, as of the time of this article download
- Access to high resolution figures
- Links to articles and content related to this article
- Copyright permission to reproduce figures and/or text from this article

[View the Full Text HTML](#)

Probing the Lewis Acid Sites and CO Catalytic Oxidation Activity of the Porous Metal–Organic Polymer [Cu(5-methylisophthalate)]

Ru-Qiang Zou,^{†,‡} Hiroaki Sakurai,[†] Song Han,[†] Rui-Qin Zhong,^{†,‡} and Qiang Xu^{*,†,‡}

National Institute of Advanced Industrial Science and Technology (AIST), Ikeda, Osaka 563-8577, and Graduate School of Science and Technology, Kobe University, Nada Ku, Kobe, Hyogo 657-8501, Japan

Received March 9, 2007; E-mail: q.xu@aist.go.jp

The oxidation of CO to CO₂ by metal catalysts has been intensively investigated; for example, gold nanoparticles have exhibited excellent properties.¹ The metal catalysts are often dispersed on a solid support, such as oxide, zeolite, and so on. Exposed to heating during vehicle use, these metal particles tend to agglomerate and grow, which causes their overall surface area to decrease. As a result, catalyst activity deteriorates.² These metal catalysts are also very easily poisoned by exposing them to moisture or organic compounds. On the other hand, the newly developed microporous metal–organic polymers (MMOPs) have recently promised many intriguing properties especially for adsorptive and catalytic applications.³ Besides the high metal content of MMOPs, one of their greatest advantages is that all active sites are homogeneous because of the highly crystalline nature of the materials.^{4,5} For optimal catalytic activity, the active sites should be freely accessible to reagent molecules, preferably via large channels or cavities.^{6,7} However, in many MOPs the metal ions are completely saturated by coordinating to the organic ligands, which makes reports on the catalytic activity of MOPs extremely scarce and little understanding of the catalytic active sites. In this Communication, we present a new MMOP, Cu(miPT) (miPT = 5-methylisophthalate), containing coordinated-unsaturated Lewis acid sites on channel walls. This MMOP material exhibits excellent and stable catalytic activity for the oxidization of CO to CO₂.⁸ ¹²C and ¹³C isotopic probe molecules are used to examine its acidity.

Treatment of an aqua solution of copper(II) nitrate and 5-methylisophthalic acid (H₂miPT) inside a Teflon capped scintillation vial at 140 °C for 4 days afforded blue block crystals [Cu(miPT)(H₂O)](H₂O)₂ (**1**). In the structure of **1**,⁹ the paddle-wheel Cu₂ clusters are interconnected by bent miPT linkers to form an undulating two-dimensional (2D) net with 4⁴ topology.^{10,11} Each copper center has a square-pyramidal coordination environment, and the two copper atoms share four carboxyl miPT ligands with an Cu–Cu interatomic separation of 2.615 Å.¹⁰ The 2D 4⁴ net consists of two kinds of calix⁴arene-like grids, where the four aromatic rings of type-I adopt a uniform cis mode while those of type-II adopt cis and trans alternate modes.¹⁰ So the type-I grid exhibits an open window with the dimensions of 8.33 × 8.33 Å² while that of type-II is self-closed to form spherical molecular cavities with a pore radius of 4.681 Å.¹⁰ The adjacent identical 2D nets are eclipsed to each other to form a microporous framework with two types of open channels (Figure 1). Interestingly, two lattice water molecules (O₂W and O₃W) and their symmetric entities by the 4-fold axis aggregate respectively into cyclic water tetramers through hydrogen-bonding interactions.¹⁰ The two types of water tetramers both assume the square conformation with an average O···O separation within the tetramer of 2.88 Å, which is comparable

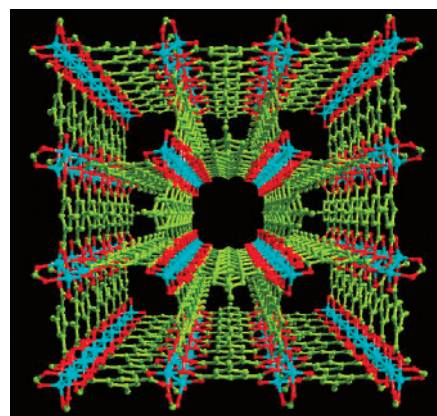


Figure 1. Perspective view of the microporous framework of **1** showing the paddle-wheel Cu₂ clusters and open channels: Cu, turquoise; C, lime; O, red.

to the corresponding value of 2.85 Å in liquid water.^{10,12} Furthermore, these water tetramers are eclipsed to each other and alternately arranged to form a 1D tube-like structure accommodated in the open channels of type-I.

Thermogravimetric analysis¹⁰ indicates that complex **1** loses the uncoordinated water molecules from 40 to 90 °C and then loses the coordinated ones from 90 to 147 °C. The host framework starts to decompose from 300 °C. The powder X-ray diffraction (PXRD) patterns illustrate that the original framework of the dehydrated **1** remains intact.¹⁰ It is interestingly noted that the dehydration of **1** is accompanied by pronounced color changes; whereas the original material is blue, the dehydrated material shows a black-violet color. Exposing the dehydrated **1** to atmosphere air, the sample restores immediately its original blue color. Furthermore, the re-adsorbed water of the materials can be easily removed by heating the sample to 150 °C in vacuum.

As compared to most of MOPs with the coordination sites blocked by the polymer-constituting ligand, complex **1** has the advantage that Lewis acid coordination sites are on the interior of the channel walls, and thus, copper sites are accessible for adsorption and catalytic conversions.⁶ Furthermore, complex **1** also possesses a percent effective free solvent volume of 29% calculated with PLATON,¹³ which offers effective space for the adsorption and catalytic conversions.

CO oxidation over **1** is performed using a fixed bed flow reactor.¹⁰ Figure 2 shows the arrhenius plot for **1** compared with our recently reported Ni-containing MOP.⁸ After activation by heating in air at 250 °C for 3 h, **1** presents a higher activity than the Ni-containing one. At 200 °C, the CO conversion over **1** reaches 100%, much higher than the reported one (3%).¹⁰ Figure 2 also shows the plots for CuO and CuO/Al₂O₃ calculated from the data in the references.¹⁴ The data shown in the figure are limited to the samples subjected to only oxidative pretreatment, because the

[†] National Institute of Advanced Industrial Science and Technology.

[‡] Kobe University.

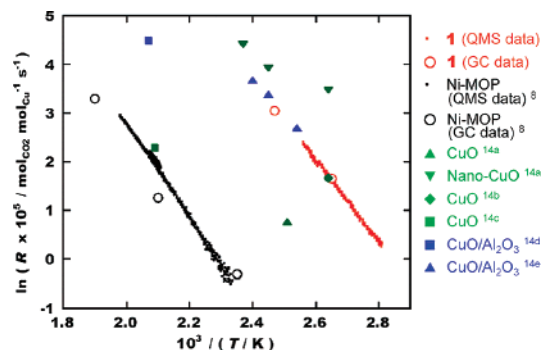


Figure 2. Arrhenius plots of CO oxidation over **1** (activated at 250 °C), the Ni-containing MOP, CuO, and CuO/Al₂O₃ catalysts.

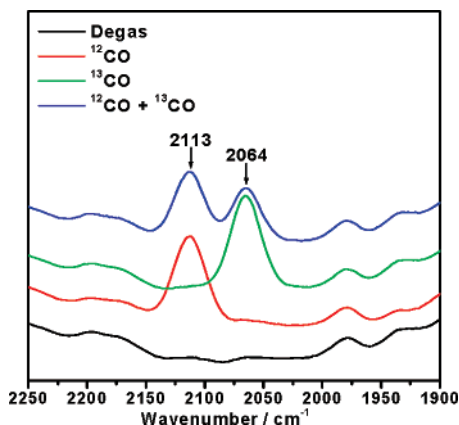


Figure 3. FTIR spectra of CO (¹²CO, ¹³CO, ¹²CO + ¹³CO) adsorbed at room temperature on **1** activated at 250 °C (2113 cm⁻¹ for ¹²CO and 2064 cm⁻¹ for ¹³CO).

activity of Cu oxide changes sensitively by the reductive pretreatment.¹⁵ The activity of **1** is similar or higher than that of CuO and CuO/Al₂O₃. The activation energy on **1** (70.1 kJ/mol) is near that of CuO (69.9 kJ/mol).¹⁶ Although room-temperature oxidation of CO is reported over CuO, the reaction is carried out under very exothermic conditions (not included in Figure 2), and the corresponding catalytic feature is lost upon exposing the sample to atmospheric air for a very short time (10–15 s).¹⁷ Although nanoCuO^{14a} showed much higher activity at 105 °C than **1**, the activity approaches a similar level to **1** above 130 °C, which may be attributed to the aggregation of nanoCuO samples at higher temperatures. It is most important that the activity of **1** is stable with time at a fixed temperature of 104 °C or higher.¹⁰ The sample of **1** also presents obstinate stability when exposed to atmospheric air. Notably, the microporous framework of **1** remains intact after removal of guest molecules and after catalytic reaction, which is indicated by the PXRD patterns.¹⁰ The elemental analysis results for both samples after removal of guest molecules and after catalytic reaction are in agreement with the theoretical value of the dehydrated sample, and in the TEM measurements no nanoCuO particles were observed,¹⁰ suggesting that the paddle-wheel Cu₂ clusters at the channel walls present the stable active sites for such catalytic oxidation.

For further confirmation of the available active site for the catalytic reaction, ¹²CO and ¹³CO probe molecules are used to examine its acid sites. Figure 3 shows the IR spectra recorded on the dehydrated **1** absorbing CO (¹²CO/Ar = 1:10, 1 atm) at room temperature. Clearly, the single bands appearing at 2113 cm⁻¹ are due to the ν(CO) vibration of CO interacting with Lewis acid sites. The isotope adsorption experiment with ¹³CO (¹³CO/Ar = 1:10, 1 atm) shows a single band at 2064 cm⁻¹, 49 cm⁻¹ red-shifted from

the ¹²CO band. The mixed ¹²CO + ¹³CO (¹²CO/¹³CO/Ar = 0.5:0.5:10, 1 atm) spectrum exhibits a sum of pure isotopic bands, suggesting the formation of mono-CO species on the Cu center. The adsorbed CO on **1** can be completely removed at 200 °C in vacuum. It should be noted that the signal at 2113 cm⁻¹ was not observed in the IR spectrum of nondehydrated **1** under the CO atmosphere, implying that CO was adsorbed inside the cavity of the dehydrated **1**, not on the bulk surface.¹⁰

In conclusion, we successfully present a new microporous MOP showing active Lewis acid sites on channel walls. The stable catalytic activity for the CO oxidation opens the door for the new-generation structurally well-defined multifunctional MOPs as catalysts for gas-phase reactions.

Acknowledgment. The authors sincerely thank the reviewers for their valuable suggestions and comments. This work was financially supported by AIST and Kobe University. R.-Q. Zou thanks JSPS for a fellowship (DC).

Supporting Information Available: Experimental procedures, analytical data, figures, and crystallographic data. This material is available free of charge via the Internet at <http://pubs.acs.org>.

References

- (1) (a) Haruta, M. *Nature* **2005**, *437*, 1098. (b) Haruta, M. *Catal. Today* **1997**, *36*, 153. (c) Haruta, M.; Kobayashi, T.; Sano, H.; Yamada, N. *Chem. Lett.* **1987**, *16*, 405. (d) Haruta, M.; Yamada, N.; Kobayashi, T.; Iijima, S. *J. Catal.* **1989**, *115*, 301. (e) Haruta, M.; Tsubota, S.; Kobayashi, T.; Kageyama, H.; Genet, M. J.; Delmon, B. *J. Catal.* **1993**, *144*, 175.
- (2) (a) Nishihata, Y.; Mizuki, J.; Akao, T.; Tanaka, H.; Uenishi, M.; Kimura, M.; Okamoto, T.; Hamada, N. *Nature* **2002**, *418*, 164. (b) Chen, M. S.; Goodman, D. W. *Science* **2004**, *306*, 252.
- (3) (a) Pan, L.; Olson, D. H.; Ciemmolowski, L. R.; Heddy, R.; Li, J. *Angew. Chem., Int. Ed.* **2006**, *45*, 616. (b) Vishnyakov, A.; Ravikovitch, P. I.; Neimark, A. V.; Buelow, M.; Wang, Q. M. *Nano Lett.* **2003**, *3*, 713. (c) Zhao, X.; Xiao, B.; Fletcher, A. J.; Thomas, K. M.; Bradshaw, D.; Rosseinsky, M. J. *Science* **2004**, *306*, 1012. (d) Rosi, N. L.; Eckert, J.; Eddaoudi, M.; Vodak, D. T.; Kim, J.; O'Keeffe, M.; Yaghi, O. M. *Science* **2003**, *300*, 1127. (e) Férey, G.; Latroche, M.; Serre, C.; Millange, F.; Loiseau, T.; Percheron-Guégan, A. *Chem. Commun.* **2003**, 2976. (f) Dybtsev, D. N.; Chun, H.; Yoon, S. H.; Kim, D.; Kim, K. *J. Am. Chem. Soc.* **2004**, *126*, 32. (g) Kesani, B.; Cui, Y.; Smith, M. R.; Bittner, E. W.; Bockrath, B. C.; Lin, W. B. *Angew. Chem., Int. Ed.* **2005**, *44*, 72. (h) Matsuda, R.; Kitaura, R.; Kitagawa, S.; Kubota, Y.; Belosludov, R. V.; Kobayashi, T. C.; Sakamoto, H.; Chiba, T.; Takata, M.; Kawazoe, Y.; Mita, Y. *Nature* **2005**, *436*, 238. (i) Kaye, S. S.; Long, J. R. *J. Am. Chem. Soc.* **2005**, *127*, 6506. (j) Dincă, M.; Dailly, A.; Liu, Y.; Brown, C. M.; Neumann, D. A.; Long, J. R. *J. Am. Chem. Soc.* **2006**, *128*, 16876.
- (4) Alaerts, L.; Séguin, E.; Poelman, H.; Thibault-Starzyk, F.; Jacobs, P. A.; De Vos, D. E. *Chem.—Eur. J.* **2006**, *12*, 7353.
- (5) (a) Wang, X.-S.; Ma, S.; Sun, D.; Parkin, S.; Zhou, H.-C. *J. Am. Chem. Soc.* **2006**, *128*, 16474. (b) Takmizawa, S.; Nakata, E.; Akatsuka, T. *Angew. Chem., Int. Ed.* **2006**, *45*, 2216. (c) Mori, W.; Takamizawa, S.; Kato, C. N.; Ohmura, T.; Sato, T. *Microporous Mesoporous Mat.* **2004**, *73*, 31. (d) Kong, L.-Y.; Zhang, Z.-H.; Zhu, H.-F.; Kawaguchi, H.; Okamura, T.; Doi, M.; Chu, Q.; Sun, W.-Y.; Ueyama, N. *Angew. Chem., Int. Ed.* **2005**, *44*, 4352.
- (6) Schlichte, K.; Kratzke, T.; Kaskel, S. *Microporous Mesoporous Mat.* **2004**, *73*, 81.
- (7) Kitagawa, S.; Noro, S.; Nakamura, T. *Chem. Commun.* **2006**, 701.
- (8) Zou, R.-Q.; Sakurai, H.; Xu, Q. *Angew. Chem., Int. Ed.* **2006**, *45*, 2542; *Angew. Chem., Int. Ed.* **2006**, *45*, 8086.
- (9) Crystal data for **1**: space group *P4/nmm*, *a* = 19.0403(7), *b* = 19.0403(7), *c* = 6.8527(4) Å; *V* = 2484.33(19) Å³, *Z* = 4, ρ_{calcd} = 1.581 g/cm³.
- (10) See Supporting Information.
- (11) Batten, S. S.; Robson, R. *Angew. Chem., Int. Ed.* **1998**, *37*, 1460.
- (12) (a) Narten, A. H.; Thiessen, W. E.; Blum, L. *Science* **1969**, *165*, 447. (b) Ma, B.-Q.; Sun, H.-L.; Gao, S. *Chem. Commun.* **2005**, 2336.
- (13) Implemented as the PLATON procedure: Spek, A. L.; *PLATON, A Multipurpose Crystallographic Tool*; Utrecht University: Utrecht, The Netherlands, 1998.
- (14) (a) Liu, W.; Flytzani-Stephanopoulos, M. *Chem. Eng. J.* **1996**, *64*, 283. (b) Skarman, B.; Grandjean, D.; Benfield, R. E.; Hintz, A. A.; Wallenberg, L. R. *J. Catal.* **2002**, *211*, 119. (c) Huang, T.-J.; Tsai, D.-H. *Catal. Lett.* **2003**, *87*, 173. (d) Huang, T.-J.; Yu, T.-C.; *Appl. Catal.* **1991**, *71*, 275. (e) Park, S.-J.; Lee, C. W.; Kim, Y.-S.; Chong, P. *J. Bull. Korean Chem. Soc.* **1995**, *16*, 183.
- (15) Huang, T.-J.; Yu, T.-C.; Chang, S.-H. *Appl. Catal.* **1989**, *52*, 157.
- (16) Jernigan, G. G.; Somorjai, G. A. *J. Catal.* **1994**, *147*, 567.
- (17) Pillai, U. R.; Deevi, S. *Appl. Catal.—B* **2006**, *64*, 146.

JA071662S